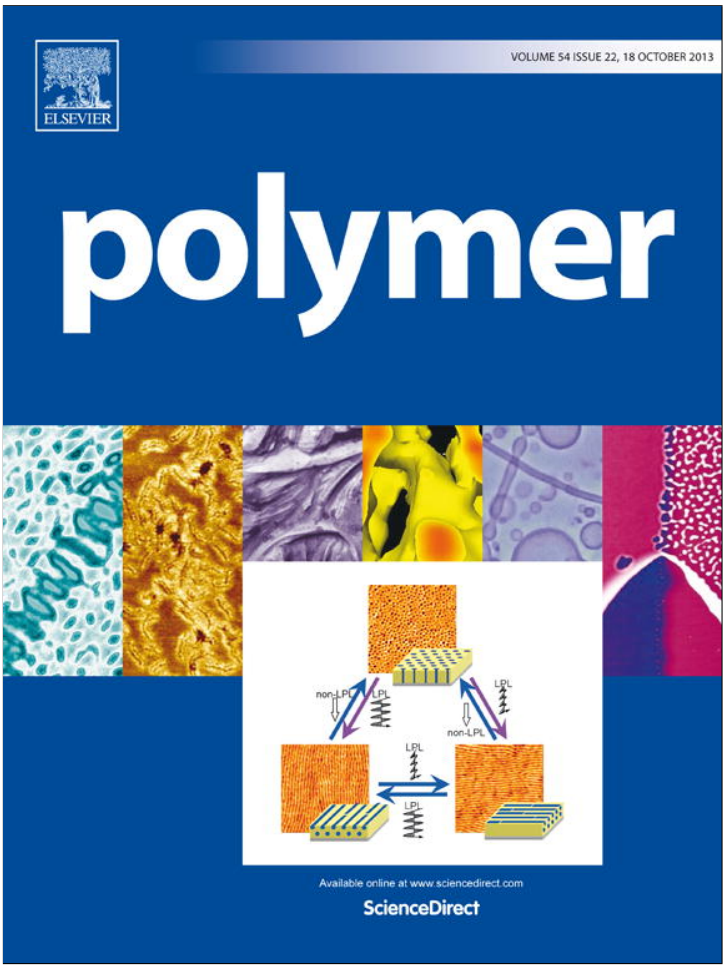

Polymer 54 (2013) 6184–6190

Contents lists available at ScienceDirect

Polymer

journal homepage: www.elsevier.com/locate/polymer

A simple strategy to generate light-responsive azobenzene-containing epoxy networks

Antonela B. Orofino [a], Gustavo Arenas [b], Ileana Zucchi [a], María J. Galante [a], Patricia A. Oyanguren [a, *]

[a] Nanostructured Polymers Group – Institute of Materials Science and Technology (INTEMA), University of Mar del Plata and National Research Council (CONICET), J. B. Justo 4302, 7600 Mar del Plata, Argentina
[b] Laser Laboratory, Department of Physics, University of Mar del Plata and National Research Council (CONICET), J.B. Justo 4302, 7600 Mar del Plata, Argentina

ARTICLE INFO

Article history:
Received 20 July 2013
Received in revised form
5 September 2013
Accepted 7 September 2013
Available online 20 September 2013

Keywords:
Epoxy networks
Azobenzene
Photoinduced anisotropy

ABSTRACT

Azobenzene containing epoxy networks are a class of photosensitive materials characterized by high thermal, optical and mechanical stability, promising for reversible optical storage applications. Here, we propose an encouraging two-step method to fabricate crosslinked coatings by simply reacting an amine-functionalized azobenzene and an epoxy resin in bulk for specified times to get soluble products (network precursors). Thin films based on these precursors were prepared, and thermally crosslinked in order to obtain high-T_g materials. The optical response of the materials was determined, both before and after crosslinking. In the case of the samples as prepared, the dynamic time response of the system is fast, as well as the relaxation of the photoinduced birefringence, as expected due to the high mobility of the chromophore. On the other hand, crosslinked systems have a slightly slower response, but higher values of remnant birefringence, providing stability of the photoinduced orientation, what makes them promising materials to use in optical storage applications. Besides, further analysis on the effect of temperature on the induced birefringence of the polymeric networks was also conducted to help optimization of material design. Finally, we had presented some preliminary investigations of surface relief grating recording in the obtained new materials.

1. Introduction

Thermoset epoxy composites are most often employed in high-performance applications because of their unique properties. Moreover, epoxy composites find new possibilities of applications, particularly when azobenzene chromophores are introduced in the formulation [1–5]. Polymers containing azobenzene units are of special interest with respect to the reversibility of the photo-orientation. The main aim of research on this kind of polymers is their utilization for optical information storage, information processing, optical switching devices and diffractive optical elements, among others [6].

For optical devices, long-term stability of the optical properties is a pre-requisite. In the case of polymeric materials for reversible optical storage, it has been reported that in high-T_g polymers, crosslinking or formation of interpenetrating polymer networks improve the thermal stability of the chromophore's orientation [7]. Thermosetting polymers may be formed in two ways: a) by polymerizing (step or chain mechanisms) monomers where at least one of them has a functionality higher than two; b) by chemically creating crosslinks between previously formed linear or branched macromolecules. The aim of this study is to explore the possibility of synthesizing azo-containing networks as thin coatings, taking advantage of the versatility of the epoxy chemistry, and using a simple two steps strategy. A second aim of this work is to evaluate if a stable photoorientation can be induced in the material and if the crosslinks have any influence on the photokinetics of the light-induced process.

This paper consists of three parts. In the first one the strategy employed for the synthesis of azo-containing networks is discussed. The second is devoted to optical response study and comparison, both before and after crosslinking. The last one concerns to preliminary investigations of surface relief grating (SRG) recording in the new materials obtained.

* Corresponding author.
E-mail addresses: poyangur@fi.mdp.edu.ar, oyangurenpatricia@gmail.com (P.A. Oyanguren).

0032-3861/$ – see front matter © 2013 Elsevier Ltd. All rights reserved.
http://dx.doi.org/10.1016/j.polymer.2013.09.008

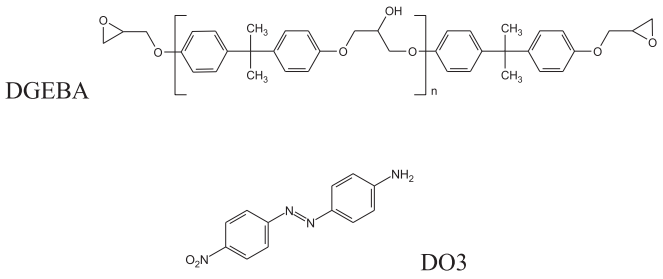

Fig. 1. Chemical structures of the materials: diglycidyl ether of bisphenol A (DGEBA), Disperse Orange 3 (DO3).

2. Experimental

2.1. Materials and sample preparation

The azo chromophore 4-(4′-nitrophenylazo)aniline (Disperse Orange 3, DO3, Aldrich, dye content 95%, Tm = 200 °C), was selected as photosensitive molecule. This is a "pseudostilbene" or "push- pull" type of azomolecule, where the 4-position and 4′-position electron-donating and electron-withdrawing groups lead to high-efficient photophysical effects. The difunctional epoxy resin employed was diglycidyl ether of bisphenol A (DGEBA, Der 332, Fluka) with a mass per mol of epoxy groups equal to 174 g mol^{-1}. Their chemical structures are shown in Fig. 1.

A series of azo-containing epoxy precursors was synthesized by the bulk reaction between DO3 and DGEBA, varying the amine/epoxy stoichiometric ratio r = (0.25–1). Reaction mixtures were prepared by mixing the monomers and cured in a convection oven at 180 °C (r = 0.25–0.75) and 190 °C (r = 1) for specified times, in order to obtain soluble products (first stage).

The precursors obtained after the first stage were dissolved in tetrahydrofuran (THF, Biopack, 99%) at a concentration of 2–5 wt% and then filtered. Films were prepared by spin coating the solutions over previously cleaned glass slides, using a single wafer spin processor (model WS-400E-6NPP-lite, by Laurell) and a spinner cycle program of 3000 rpm for 60 s. The films thicknesses were varied (in the range of 100–200 nm) by adjusting the concentration of the solution. They were determined with a perfilometer Tencor D100, sensing the height difference between the film and the glass substrate, across a scratch made in the sample. Once prepared, the samples were subjected to thermal treatment at 180 °C (r = 0.25–0.75) and 190 °C (r = 1) in a convection oven during the time required for each formulation to attain complete conversion of epoxy monomer (second stage of curing).

2.2. Characterization techniques

Fourier transform infrared spectroscopy (FTIR) was performed using a Thermo Scientific Nicolet 6700 Spectrometer (4 cm^{-1} resolution), provided with a heated transmission cell (HT-32, Spectra Tech) and a programmable temperature controller (CAL 9500P, Spectra Tech, $\Delta T = \pm$ 0.1 °C). Reactive mixtures were placed between two glass covers separated 2 mm.

Differential scanning calorimetry (DSC, Pyris 1 Perkin Elmer) was used to determine thermal transitions of precursors and networks. Dynamic scans were performed under nitrogen flow at 10 °C min^{-1}, and the glass transition temperature (T_g) was defined at the onset of the change in specific heat.

Thermogravimetric tests were performed in a TGA-50 SHIMADZU Thermogravimetric Analyzer. About 9.0 mg samples were put in an alumina crucible and heated from 40 to 700 °C at a heating rate of 10 °C min^{-1} under air atmosphere.

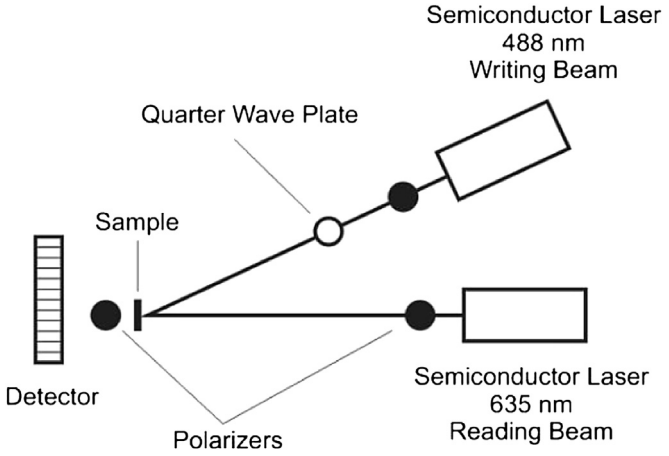

Fig. 2. Experimental setup to measure photoinduced birefringence.

Photoinduced birefringence of the resulting films was determined using the experimental setup described in Fig. 2. Birefringence was measured by placing the samples between two crossed linear polarizers. A semiconductor laser at 488 nm (Coherent SapphireTM 488-20 OEM Laser) was used as a writing beam to induce optical anisotropy in the polymer film, and another semiconductor laser at 635 nm (laser diode, model I-R-5-P) was used as a reading beam, measuring the power that is transmitted through this optical setup with a photodiode. To achieve the maximum signal, the polarization vector of the writing beam is set to 45° with respect to the polarization vector of the reading beam. All measurements were performed at room temperature and all the films were irradiated with 4 mW mm^{-2} of the writing laser.

The induced optical birefringence (Δn) is determined by measuring the reading beam transmission ($T = I/I_0$) using the relation:

$$\Delta n = (\lambda/\pi d)\sin^{-1}(I/I_0)^{1/2} \quad (1)$$

where λ is the wavelength of the incident radiation, d is the film thickness, I_0 is the incident beam intensity and I is the intensity after the second polarizer. In order to erase the photoinduced birefringence, a removable quarter wave plate was used to induce circular polarization in the 488 nm laser, in this case being the erasing beam.

To evaluate the stability of the photoinduced birefringence, the optical response of polymeric networks subjected to temperature was followed. Samples were placed in a heated transmission cell (HT-32 Spectra Tech) provided with a programmable temperature controller (Omega, Spectra Tech, ±1 °C) in the same configuration of the optical system. Temperature of the samples was measured very carefully with an exposed-juncture thermocouple (CHY 501 K Thermometer, ±0.1 °C), on the same spot being irradiated, but on the clean side of the glass slide, to avoid sensing the furnace temperature instead.

The recording of the gratings was performed at room temperature with a p-polarized laser beam (λ = 488 nm), with a power of 10 mW. The interference pattern was created using the Lloyd mirror configuration: half of the beam was incident on the sample, and the other half was reflected from a mirror set at the right angle with the sample to coincide with the direct beam [8]. The fringe spacing Λ was determined by the angle between the beam propagation axis and the sample normal θ, as:

$$\Lambda = \lambda/(2\sin\theta) \quad (2)$$

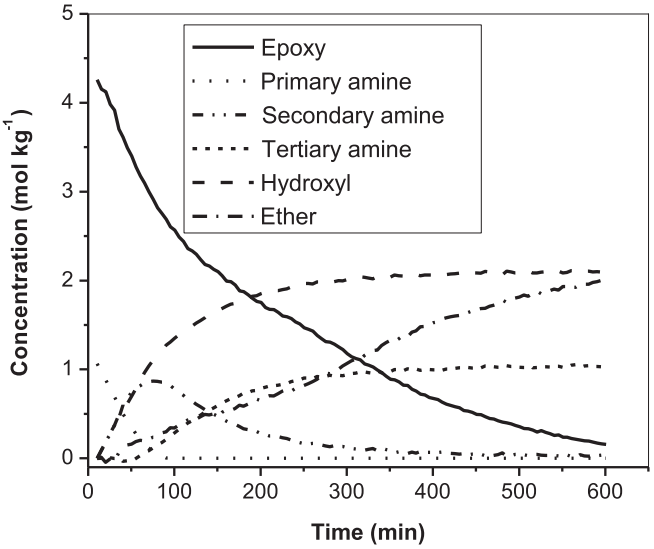

Fig. 3. Evolution of epoxy, hydroxyl, ether and amine groups concentration during reaction as a function of time for a formulation with $r = 0.50$.

where λ is the writing wavelength laser. Here, the spacing was set to approximately 1 μm. Exposure time was set to nearly 20 min. The modulation depth of the final inscribed surface relief gratings was measured by atomic force microscopy (AFM, Agilent 5500 SPM).

3. Results and discussion

The curing kinetics of epoxy resins with amines as hardeners has been well investigated. There are three basic reactions occurring during curing: (a) the epoxy group reacts with a primary amine to produce a secondary amine, (b) the epoxy group reacts with a secondary amine to produce a tertiary amine, and (c) secondary reactions, such as etherification and homopolymerization of the epoxy group, resulting in the formation of an ether linkage [9]. Usually when the concentration of epoxy groups is equal to or lower than the concentration of amine groups, side reactions do not take place. When there is an excess of epoxy groups or when the secondary amino groups have a low reactivity, the epoxy–hydroxyl reaction (etherification) can compete with the two previous ones. Moreover, the homopolymerization reaction of the epoxy resin can occur at high temperatures, and can be initiated by impurities or by tertiary amine groups. Epoxy monomers polymerize through step-growth, (a) and (b), and chain-growth (c) processes. These different reaction mechanisms make it possible for reactive mixtures to undergo two-step polymerization. Firstable, azo-containing epoxy prepolymers are obtained by step-growth polymerization of two difunctional monomers: epoxy (in excess) and azo-amine. The reaction of these prepolymers is then thermally initialized and crosslinked via chain polymerization of the epoxy units present in the extreme of the oligomers and hydroxyl groups, leading to three-dimensional networks.

The knowledge of the curing kinetics: reaction rate and how this rate changes with curing temperature is important and useful to predict the chemical conversion achieved after a curing schedule. A standard method [10,11] was used to calculate the changes in concentration of epoxy, hydroxyl, ether and amine groups (primary, secondary and tertiary) during curing. Reactions were studied via *in situ* FTIR spectroscopy, using conversion data for epoxy and primary amine groups, the deconvolution of the area of the overlapped peaks for primary amine (6652 cm^{-1}) and secondary amine (6662 cm^{-1}), and mass balances to calculate concentration of all species. The reference band was 4623 cm^{-1} [12]. For instance, in Fig. 3 it is shown the evolution of the concentration of the different groups (epoxy, ether, hydroxyl, and amines) for the formulation with $r = 0.50$. Previous studies were done on a similar system which led to reaction products with epoxy groups in the extreme of chains [12]. The optimum polymerization time for the first stage was reported as the intersection of the concentrations of primary amine and ether groups. Using this curing time the synthesized prepolymer could subsequently be dissolved, avoiding further extent of the etherification reaction. This criterium was used to select the reaction times for the first stage, both in bulk and in thin films, giving soluble products in all the cases. These time values are shown in Table 1, middle column, for all the formulations studied.

Table 1
Reaction times of the two stages of curing at 180 °C for formulations with $r < 1$ and 190 °C for the formulation with $r = 1$.

Formulation	First stage reaction time (min)	Second stage reaction time (min)
$r = 0.25$	75	720
$r = 0.50$	60	420
$r = 0.75$	45	300
$r = 1$	30	120

Further thermal treatment (second stage) leads to the development of an irreversible crosslinking process. It was observed that during this stage of curing the thermally induced reactions result in a partial degradation of the azo chromophores. With the aim of optimizing reaction times of this stage, a detailed study on the evolution of the films during curing was performed, registering their UV spectra, thermogravimetric behavior and optical response. Fig. 4a–b shows the dependence of the maximum photoinduced birefringence as well as the amount of stored information (remnant birefringence, RB), with curing time during crosslinking. As can be observed there, the remnant birefringence achieved is practically the same and remains constant for all the films. However, an optimum time, for which the maximum value of anisotropy is reached, exists for each formulation. The initial increase in the birefringence of the samples is related to a significant shrinkage of the films during curing. The thickness ratio of the film at any time, T_t, to the initial thickness of the film, T_0, as a function of curing time, which provides a measurement of the shrinkage during crosslinking, can be appreciated in Fig. 4c. After reaching a maximum, the photoinduced birefringence decreases with curing time. This unusual behavior is probably caused by the gradual degradation of azo chromophores. To confirm this assumption, UV–visible spectra were recorded for each composition at different curing times. For instance, Fig. 5 shows the absorption spectra of a film prepared with $r = 0.50$ at selected curing times. The absorption spectra exhibit a systematic decrease of the absorption maxima. As increasing the time of curing, it is also observed a shift of the absorption maxima to shorter wavelength accompanied by a slight broadening of the band. For this formulation the time at which the peak of the film shifts, as evidenced in the spectrum for 10 h at 180 °C, coincides with the one at which the photoinduced birefringence also decreases (see Fig. 4a). Based on these experimental data, the time for the maximum birefringence (minimum thickness and minimum degradation simultaneously) is considered the optimum curing time for each composition. Curing times for the second stage are shown in the third column of Table 1. To analyze the thermogravimetric behavior of the films during the second stage, a sample with $r = 0.5$ was kept in the TGA at 180 °C for 420 min. During this period a weight loss of only 1.5% was developed (see Supporting Information).

The efficiency of the crosslinking was confirmed by evaluation of the solubility behavior in THF, a good solvent for azo-containing

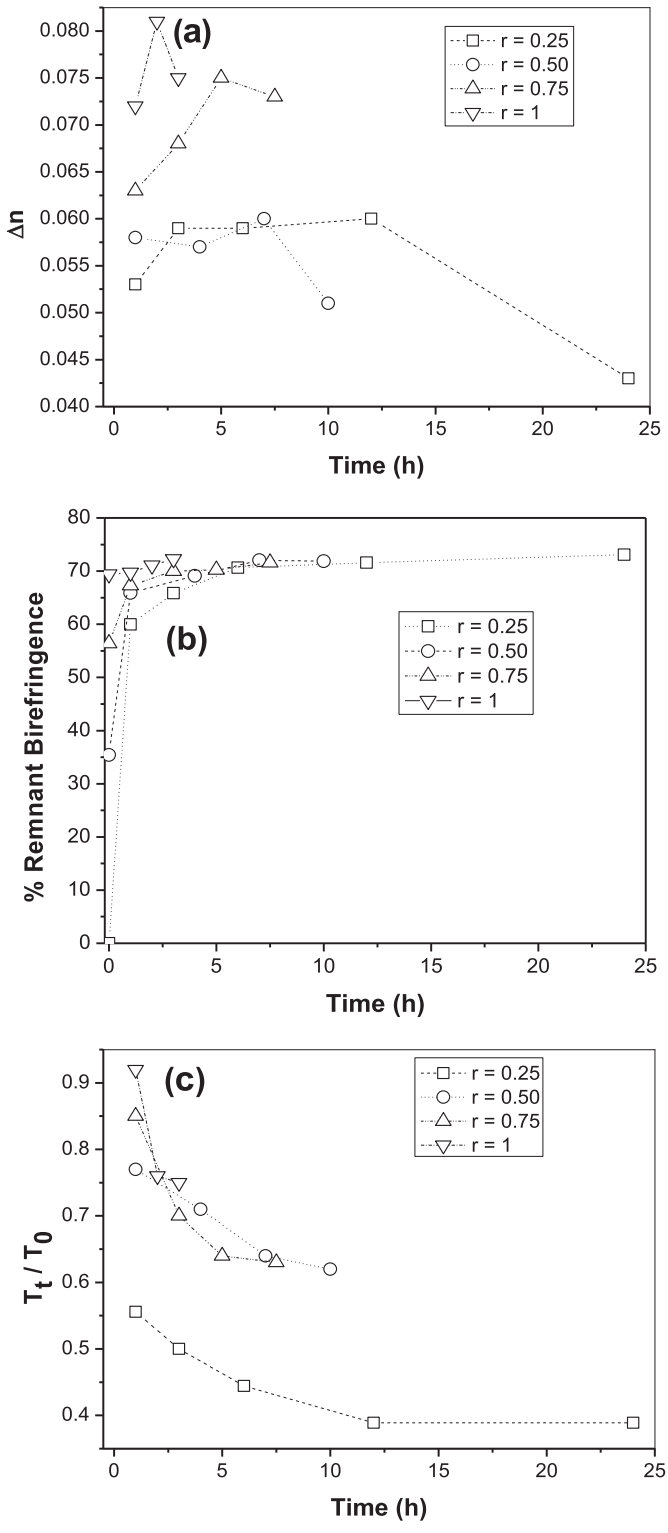

Fig. 4. Evolution of: (a) maximum photoinduced birefringence, (b) percentage of remnant birefringence, and (c) shrinkage, expressed in terms of the thickness ratio of the film at any time, T_t, to the initial thickness of the film, T_0; with curing time during crosslinking at 180 °C for formulations with $r < 1$ and 190 °C for the formulation with $r = 1$.

epoxy precursors. As expected, a film prepared using the precursors was completely washed out the glass substrate. However, by visual inspection of the rinsed crosslinked film, no species containing azo chromophore belonging to the sol fraction were observed,

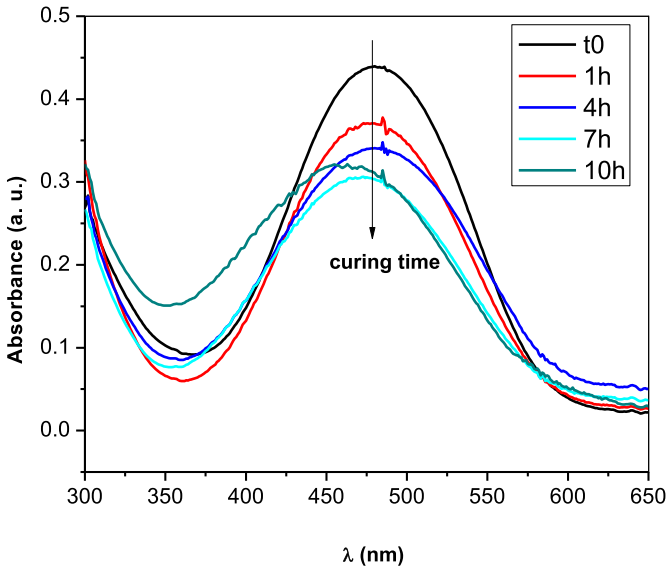

Fig. 5. UV–visible spectra for a formulation with $r = 0.50$ taken at different times of curing at 180 °C.

confirming that all species that contain azobenzene moieties were forming part of the gel. Thus the initially well-soluble film becomes insoluble because of reaction.

The motion of the azo group, and thus its orientation, could be affected by the crosslinking of the molecular environment. The photoinduced isomerization cycles may be expected to depend more strongly on the molecular arrangement of the environment. This fact can have a double effect on photoorientation: it restricts the chromophore's motion, making it harder to induce orientation (this means slower rates of birefringence growth), but it also confers better stability upon induced anisotropy after the light is turned off. Typical writing–relaxing–erasing curves (irradiation/switch off/circularly polarized light on) of optically induced and subsequently removed birefringence of films before and after crosslinking, are shown in Fig. 6. Characteristic parameters for all the systems under study are summarized in Table 2.

As shown in Fig. 6, the birefringence in both types of samples (before and after crosslinking) is induced rapidly with the irradiation of the linearly polarized laser. For the uncrosslinked samples, (except the $r = 0.25$ one, whose T_g was below ambient temperature and did not show photoinduced birefringence) the dynamic response of the system, characterized by the time necessary to achieve 80% of the saturation signal, were fast in general. This fast writing speed is expected due to the high mobility of the chromophore. This effect is also noted on the remnant birefringence values, which are directly related to the T_g values of the polymers. Increasing T_g leads to an increase in the stored information. One can assume that the mobility of the azo chromophore is much higher when the glass transition temperature of the material is lower. For the crosslinked samples, all the formulations showed a significant increase in their T_g. In addition, crosslinking restrains the mobility of oriented azo groups for randomization, thus providing stability of the photoinduced orientation. Both effects, higher T_g and crosslinks, are perceived as an increase in the amount of remnant birefringence. As we have already discussed, the level of anisotropy stored is approximately the same for all the compositions analyzed (Fig. 4b). For the same reason response times are longer than before crosslinking, (especially for $r = 0.25$) but are still reasonable for practical applications. For $r = 1$, in spite of the fact that the T_g increases after crosslinking, there are no significant improvement over the remnant birefringence; it raises less than 3%, meanwhile

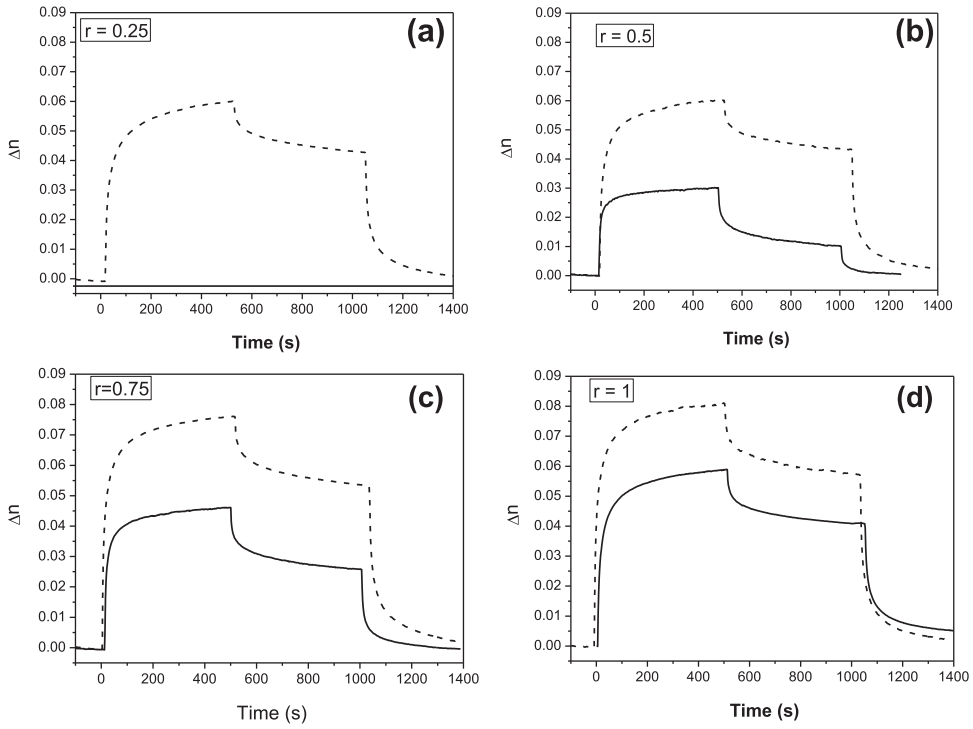

Fig. 6. Time evolution of the photoinduced birefringence showing typical writing–relaxing–erasing cycles for samples before (solid line) and after crosslinking (dashed line) for different formulations: (a) $r = 0.25$, (b) $r = 0.50$, (c) $r = 0.75$, and (d) $r = 1$.

the response time is 13 s longer. When comparing the different systems, another variable to take into account is the synthesis time, as the sum of both steps. For example, samples prepared with $r = 0.25$ and 0.75 differ in 20 h when curing at high temperature (25–5 h at 180 °C), obtaining a 5% increase in remnant birefringence, as well as a raise in the response time of 42 s. The results depicted in Fig. 6 and Table 2 demonstrate that the crosslinks obviously cause a slowing down of the kinetics of photoorientation and an important increase in the stability of the photoinduced anisotropy. It means that, the synthesized networks are coarse enough for the molecular motion needed for the photoisomerization of azobenzene groups.

Fig. 7 shows the maximum birefringence with chromophore concentration of all the films, before and after crosslinking. For uncrosslinked samples there is a linear increase in the birefringence level as the azo group content increased. On the other hand, crosslinked films seem to be capable of storing information with remarkably high values for the photoinduced birefringence. For these films the maximum birefringence also increases with the azo content, but for all the formulations analyzed the maximum values are much higher than the expected based on their chromophore content. This behavior can be interpreted on the basis of the differences in the chemical structures of the materials analyzed. In a previous publication [5], we have shown that the level of maximum birefringence that can be achieved in a crosslinked epoxy-based azo-polymer was about 0.03 for 24 wt% DO3. It was demonstrated that the photoorientation of the azo chromophores was not influenced by the crosslinking itself but that it depended rather on the local free volume distribution around the chromophores. As the azo chromophore was not forming part of the bridges between the polymer chains, it had a rather high mobility in the free volume of

Table 2
Thermal and optical properties of samples before and after crosslinking.

Formulation	% DO3	Bulk T_g (°C)	% RB[a]	t 80% (sec)[b]	Δn
Uncrosslinked samples					
$r = 0.25$	14.8	−6.6	–	–	–
$r = 0.50$	25.8	24.1	35.4	29	0.032
$r = 0.75$	34.2	50.3	56.4	39	0.044
$r = 1$	41.0	76.1	69.4	64	0.048
Crosslinked samples					
$r = 0.25$	14.8	112.1	71.6	117	0.060
$r = 0.50$	25.8	116.4	72.0	74	0.060
$r = 0.75$	34.2	125.0	71.6	75	0.075
$r = 1$	41.0	112.7	71.1	77	0.081

[a] Remnant birefringence.
[b] Time to achieve 80% of the saturation level.

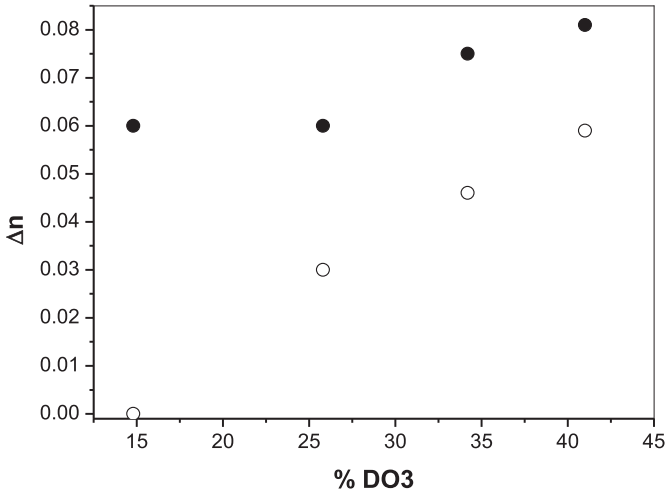

Fig. 7. Maximum birefringence of films before (open circle) and after (filled circle) crosslinking as a function of chromophore concentration.

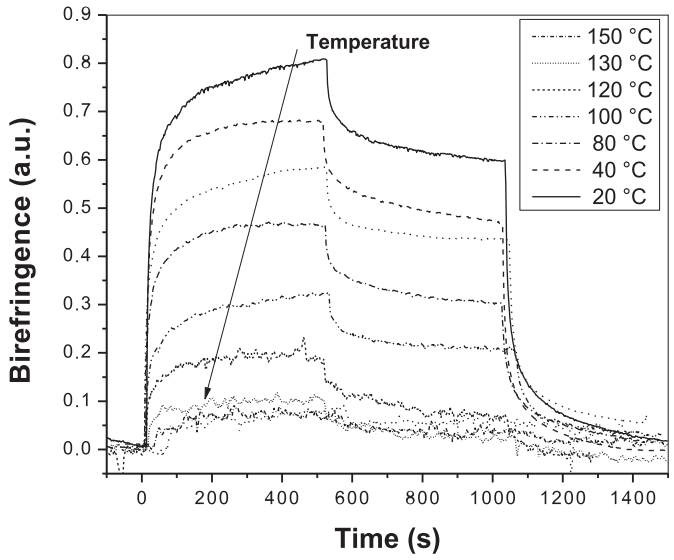

Fig. 8. Photoinduced birefringence as a function of time at different temperatures for an azo-network film with $r = 0.75$.

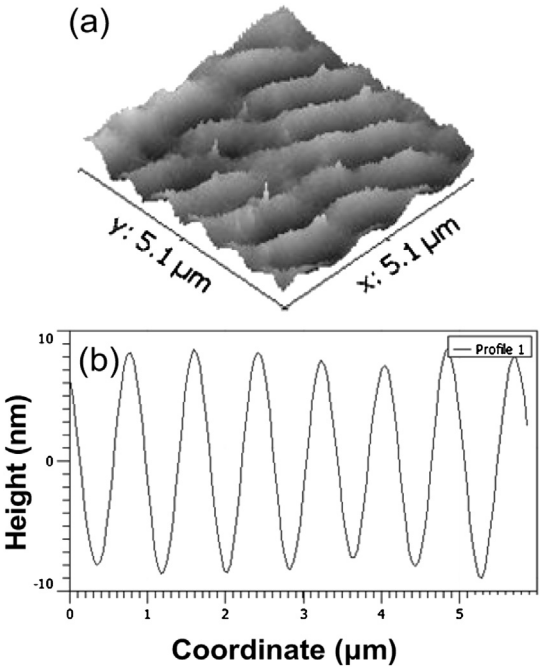

Fig. 9. (a) AFM image and (b) surface profile of gratings inscribed into the azo-polymer network surface. Film thickness = 110 nm for a formulation with $r = 0.75$.

the azo network. Similar results were obtained for crosslinkable polymethacrylates containing azobenzene and acrylic groups on separate side chains in order to maintain an adequate azo mobility in the networks [13]. Comparing the present networks with the previously reported [5] the main difference consists in the presence of crosslinks that affect the mobility of azo chromophores. In an epoxy-amine mixture, primary amine-epoxy and secondary amine-epoxy reactions during precursors formation (stage 1) yield new hydroxyl groups. These secondary hydroxyls present in the precursors suffer chain-transfer reactions during anionic epoxy homopolymerization [14], changing the network architecture. Then, based on the reported values of birefringence levels for amorphous polymers, the birefringence levels achieved in the present study are the expected for uncrosslinked films and very high for crosslinked ones.

The effects of external parameters on photoinduced anisotropy have also been investigated. The effect of temperature on the birefringence is shown in Fig. 8 for a crosslinked 110 nm-thick film prepared with $r = 0.75$. Increasing the temperature results in a loss of orientation for azo moieties because of the high mobility of both chromophore and crosslinked matrix. It is expectable that when the temperature reaches T_g, the alignment is lost as the chromophores restore their isotropic distribution [15]. The bulk T_g for this formulation is 125 °C (Table 2), however, at 150 °C a certain level of birefringence is still observed. This behavior is probably related with a substantial shift of the film dynamics compared to bulk samples, evidently related to thin-film confinement. Yager et al. [16] reported that the deviation from bulk T_g becomes very large in thin films. For instance, for a film of ~50 nm thickness the measured T_g results ~50 °C higher than the bulk glass transition.

Thermal stability of crosslinked films was evaluated from thermogravimetric analysis (see Supporting Information). A general observation is that the thermogravimetric curves are quite similar for all the samples and that degradation takes place in three steps. It starts from 265 °C and the rates of weight loss are maximal at 290, 400 and 650 °C. The weight loss corresponding to the first step is low (13–15%), while the last step leads to a complete degradation of the material. Similar results were reported by Bellenger et al. [17] who compared the thermogravimetric behaviors of some several epoxy amine systems. They have shown that amine-cured epoxy resins undergo radical chain oxidation, leading to the transformation of amine to amide groups during the first step. The consequence of this reaction is to prevent nucleophilic chain scissions near the nitrogen atom and the formation of thermolabile structures. For the thermosets synthesized here, epoxy prepolymers are first obtained by step-growth polymerization of two difunctional monomers: epoxy (in excess) and azo-amine. The reaction of these prepolymers is then thermally initialized and crosslinked via chain polymerization of the epoxy units present in the extreme of the oligomers and hydroxyl groups, leading to three-dimensional networks. So, the first degradation step is probable due to the transformation amine → amide. This assumption is based on the experimental result that shows that when increasing azobenzene content the weight losses corresponding to the first degradation step are higher. At 650 °C, random scission of the three-dimensional network probably occurs, which is relatively little influenced by the structure.

Efficient SRG formation in the epoxy-based low molecular weight azo-polymer films has already been demonstrated [18]. Published data [19,20] show that the presence of azo groups is a critical structural requirement for such effect as no SRG could be inscribed on systems containing other photochromic groups. This surface patterning phenomenon still lacks a satisfactory explanation, despite extensive research. Barret et al. [21] reported their results of PMMA of variable molecular weight blended with poly-Disperse Red 1 acrylate and showed that when molecular weights are increased above those of the azo homopolymers (but below the limit of entanglement), there is a decrease in both the inscription rate and grating depth achievable, up to a point where phototransport is prevented by the high viscosity of the entangled bulk polymer. Based on this knowledge and that the networks synthesized here have a high crosslink density, these crosslinks are expected to restrict surface initiated material movement and hence the grating formation.

As shown in Fig. 9, a well-defined surface relief grating could be inscribed in the azo material. The periodicity of the grating is diffraction limited, being determined by the wavelength of light

and the inscription geometry. The grating spacing is consistent with the theoretically calculated (Equation (1)), using an angle $\theta = 17^{\circ}$ a peak-to-peak spacing of 830 nm was obtained. The surface modulation depth was about 16 nm for a film thickness of 110 nm, as it is shown in Fig. 9b.

The relief grating formation process is found to be strongly dependent on the nature of the surface (especially the top 'skin layer' with the thickness of 2–20 nm), while the birefringence grating appears to be a purely bulk process. Formation of the SRG pattern requires rearrangement of polymer molecules (at least locally at a segmental level) and therefore significant chain mobility. One can make a distinction of at least three different layers within the film thickness: an interfacial layer contacting the substrate, a surface layer contacting with air, and an intermediate ('bulk') layer between them. Different polymer chain mobilities are expected for these three layers. While the interfacial layer chains are restricted because of their interaction with the substrate, the surface layer chains are highly mobile and can easily change their conformation or diffuse on the surface. Thicker films obviously have a larger portion of the macromolecules constituting the surface and the intermediate layers. Kulikovska et al. [22] studied the formation of surface relief gratings as a function of film thickness for several polyacrylic-backbone polymers with azobenzene pendant groups. They found that SRG modulation depth is affected by the film thickness and is found to increase with it. Specifically, ultrathin films (less than 100 nm in thickness) are typically characterized with a flat surface while when the film thickness exceeds 500 nm, no noticeable changes in the SRG depth with thickness are observed. Taking these considerations into account, the detected surface modulation in the crosslinked film studied here results reasonable.

4. Conclusions

In summary, we had successfully generated a feasible method to fabricate photosensitive crosslinked coatings characterized by very high thermal, optical, and mechanical stability. Thin films of this insoluble epoxy network can be obtained by spin coating of soluble azobenzene containing precursors and an additional thermal treatment, yielding a recording material of high T_g. Moreover, it was demonstrated that the presence of crosslinks plays an important role in the stability of the photoinduced orientation. Volume gratings could be laser inscribed in crosslinked azopolymer thin films. This feature combined with high thermal, optical and mechanical stability makes these materials promising candidate to be used in photonic applications.

Acknowledgments

The authors thank the financial support of the following Argentine institutions: University of Mar del Plata, National Research Council (CONICET), and National Agency for the Promotion of Science and Technology (ANPCyT).

Appendix A. Supplementary data

Supplementary data related to this article can be found at http://dx.doi.org/10.1016/j.polymer.2013.09.008.

References

[1] Schab-Balcerzak E, Janeczek H, Kaczmarczyk B, Bednarski H, Sek D, Miniewicz A. Polymer 2004;45:2483.
[2] He Y, Yin J, Che P, Wang X. Eur Polym J 2006;42:292.
[3] Kim DY, Tripathy SK, Li L, Kumar J. J Appl Phys Lett 1995;66:1166.
[4] He Y, Wang X, Zhou Q. Polymer 2002;43:7325.
[5] Fernández R, Mondragón I, Galante MJ, Oyanguren PA. J Polym Sci Part B Polym Phys 2009;47:1004.
[6] Natansohn A, Rochon P. Adv Mater 1999;11:1387.
[7] Takase H, Natansohn A, Rochon P. Polymer 2003;44:7345.
[8] Mai X, Moshrefzadeh R, Gibson UJ, Stegeman GI, Seaton CT. Appl Opt 1985;24:3155.
[9] Pascault JP, Williams RJJ. General concepts about epoxy polymers. In: Pascault JP, Williams RJJ, editors. Epoxy polymers. Weinheim: WILEY-VCH Verlag GmbH & Co; 2010. p. 1–12.
[10] St John N, George GA. Polymer 1992;33:2679.
[11] Xu L, Fu JH, Schlup JR. Ind Eng Chem Res 1996;35:963.
[12] Fernández R, Blanco M, Galante MJ, Oyanguren PA, Mondragon I. J Appl Polym Sci 2009;112:2999.
[13] Takase H, Natansohn A, Rochon P. J Polym Sci Part B Polym Phys 2001;39:1686.
[14] Dell'Erba IE, Williams RJJ. Polym Eng Sci 2006;46:351.
[15] Cojocariu C, Rochon P. Pure Appl Chem 2004;76:1479.
[16] Yager KG, Barrett CJ. J Chem Phys 2007;126:94908.
[17] Bellenger V, Fontaine E, Fleishmann A, Saporito J, Verdu J. Polym Degrad Stab 1984;9:195.
[18] Goldenberg LM, Kulikovsky L, Gritsai Y, Kulikovska O, Tomczyk J, Stumpe J. J Mat Chem 2010;20:9161.
[19] Barret CJ, Natansohn A, Rochon P. J Chem Phys 1998;109:1505.
[20] Viswanathan NK, Kim DY, Bian S, Williams J, Liu W, Li L, et al. J Mater Chem 1999;9:1941.
[21] Barrett CJ, Natansohn A. J Phys Chem 1996;100:8836.
[22] Kulikovska O, Gharagozloo-Hubmann K, Stumpe J, Huey BD, Bliznyuk VN. Nanotechnology 2012;23:485309.